

Geometry and Cenozoic evolution of the Crimean fold-thrust belt from cross-section balancing and kinematic forward modeling

© M. Nakapelyukh^{1, 2}, V. Belskyi³, L. Ratschbacher², 2018

¹Subbotin Institute of Geophysics, National Academy of Sciences of Ukraine, Kiev, Ukraine

²Freiberg University of Mining and Technology, Freiberg, Germany

³Institute of Geochemistry, Mineralogy and Ore Formation,
National Academy of Sciences of Ukraine, Kiev, Ukraine

Received 15 February 2018

Кримський складчасто-насувний пояс складається з Кримського куполоподібного складчастого поясу та акреційного клину Сорокіна з високими перспективами на нафту і газ. Поєднано геоморфологічний аналіз і метод балансування геологічних розрізів, опубліковані низькотемпературні термохронологічні дані та дані акваторіальних сейсмічних профілей для відтворення як сучасної будови, так і кайнозойської структурної еволюції. Інтерпретовано Кримський купол як антиформну структуру в масштабі карти, що пов'язана з головним кримським насувом (базальним детачментом для гірської частини складчастого поясу). Головний кримський насув відділяє континентальну Скіфську плиту від перехідної океанічної Східночорноморського басейну і, ймовірно, реактивує структуру пасивної континентальної окраїни верхнього тріасу—нижньої юри. Кримський складчасто-насувний пояс зазнав ~24 км скорочення, починаючи з еоцену, з приблизно однаковим скороченням (~12 км) в обох структурах — Кримському куполі та Сорокінському акреційному клині. Проміжні стадії деформації, прослідковані кінематичною форвард-моделлю, є предметом перевірки майбутніми пошуками вуглеводнів і термохронологічними дослідженнями.

Ключові слова: Кримський складчасто-насувний пояс, товстошарова і тонкошарова структурна геометрія, збалансований перетин, кінематичне пряме моделювання.

Introduction. The geology of the Crimean peninsula records the interaction between the Eastern Black-Sea basin and the Scythian platform as the result of the Arabia-Eurasia collision [Saintot et al., 1999; Nikishin et al., 2001; Mileev et al., 2006]. Although the region has been studied for more than a century, the localization, geometry, and amount of deformation in the fold-thrust belt in the on- and offshore parts of the peninsula are avidly debated and remain to be fully understood (e. g. [Favre, 1877; Foht, 1926; Muratov, 1960; Muratov, Sydorenko, 1969; Kazantsev, 1982; Slavin, 1989; Nikishin et al., 2001, 2003]). Onshore, new biostratigraphic studies indicate the existence of at least two lithostratigraphical

units comprising turbidites ("flysch"), formed in the Upper Triassic—Lower/Middle(?) Jurassic and the Upper Jurassic—Lower Cretaceous during continental margin and back-arc rift formation, respectively [Nikishin et al., 2015c; Sheremet et al., 2016a; Oszczypko et al., 2017]. These studies provided a better regional correlation of the Mesozoic strata, which allows the reconstruction of the Cenozoic deformation in the Crimean fold-thrust belt along the southern rim of the peninsular. Offshore, seismic profiles detailed the structures of the Sorokin accretionary wedge and its transition to the onshore structures [Nikishin et al., 2015a, b; Sheremet et al., 2016b; Sydorenko et al., 2016]

In this study, we present a balanced cross section and a kinematic forward model for the Crimean fold-thrust belt. Our analysis reveals thick- and thin-skinned deformation geometries in the onshore—offshore transition, which are related to the northwestward subduction of the Eastern Black-Sea basin under the Scythian platform. The moderate shortening in the Scythian platform sedimentary cover preserved key features for the restoration of the structural geometry, i.e., the flat Upper Cretaceous—Lower Eocene strata atop a vast upper Albian peneplain, which allows the tracing the subsequent Cenozoic folding and faulting.

Geological setting. Between the Black-Sea basin and the Scythian plate, the Crimean peninsula fold-thrust belt and the Western Greater Caucasus accommodate the convergence between Arabia and Eurasia (Fig. 1) [Saintot et al., 1999; Stephenson et al., 2004]. The Scythian plate comprises the stretched continental margin of the East European platform [Khain, 1984; Kruglov, Tsypko, 1988; Kazantsev, 1982; Stephenson et al., 2004; Saintot et al., 2006; Meijers, Vrouwe, 2010]. The Black Sea basin consists of two sub-basins — the Eastern Black Sea and the Western Black Sea — Mid Black Sea Ridge. These sub-basins opened mainly during the Lower Cretaceous as back-arc basins behind the Pontide subduction zone with both sub-oceanic and thinned continental lithosphere; they feature large-displacement normal faults [Robinson et al., 1996; Nikishin et al., 2003, 2015b,c]. In the south, renewed extension took place during the latest Cretaceous—Paleogene, whereas in the north — along the southern rim of the Scythian plate-tectonic quiescence followed the Lower Cretaceous rifting [Khriachtchevskaia et al., 2010]. McClusky et al. [2000] suggested that the transitional and oceanic lithosphere underlying the Black Sea is rheologically stronger than the continental lithosphere to its north and south. On the one hand, the basin has been acting as a backstop, resisting deformation and focusing it in the adjacent continental lithosphere. On the other hand, the rigid back-arc basin lithosphere has transferred deformation over

large distances, causing — for example — the shortening in the north of the Western Black Sea basin [Munteanu et al., 2013]. There, thrusting inverted the Cretaceous rift margin of the Odessa shelf, causing ≤ 16 km shortening (Fig. 1, *b*) [Munteanu et al., 2011].

In the Greater Caucasus, olistostromes and a regional angular unconformity record Eocene to Oligocene deformation that occurred as a far-field response to the initiation of the continental collision between the Arabian and Eurasian plates (see Fig. 1, *b*) (e. g. [Robinson et al., 1996; Vincent et al., 2007]). The central portion of the Greater Caucasus yielded Paleogene to Pliocene low-temperature thermochronologic ages; most of the exhumation was post-Miocene [Kral, Gurbanov, 1996; Avdeev, Niemi, 2011]. Deformation along the Western Greater Caucasus accommodated Cenozoic dextrally transpressive deformation between the Eastern Black-Sea basin and the Scythian plate. There, post-Eocene exhumation decreases from southeast to northwest from ~ 7 km to < 5 km [Vincent et al., 2010; Avdeev, Niemi, 2011]. The Odessa and Western Crimean sinistral strike-slip faults indicate a northwestward propagation of the East Black-Sea basin and northwest—southeast shortening across the southern rim of the Crimean peninsula. There, the Crimean fold-thrust belt developed, which contains an onshore part — the Crimean dome — and an offshore part — the Sorokin accretionary wedge, separated by the Main Crimean thrust (Fig. 2, *a*). In this belt, both low-temperature geochronology [Pánek et al., 2009] and stratigraphy [Nikishin et al., 2015c] indicate that the shortening commenced in the Eocene. An elastic block model, derived from the present-day plate motions, predicts 0,6—1,3 mm/year dextral strike-slip shear between the Eastern Black-Sea basin and the Scythian plate (Fig. 1, *b, c*) [Reilinger et al., 2006]; earthquakes in the Crimean fold-thrust belt witness this active deformation (see Fig. 2, *a*).

For the purpose of this study, we interpreted the stratigraphy of the Crimean peninsula and the adjacent Black-Sea basin to reflect three evolutionary stages (Fig. 2, *a, 3*). 1. The pre-Albian rocks represent the crystal-

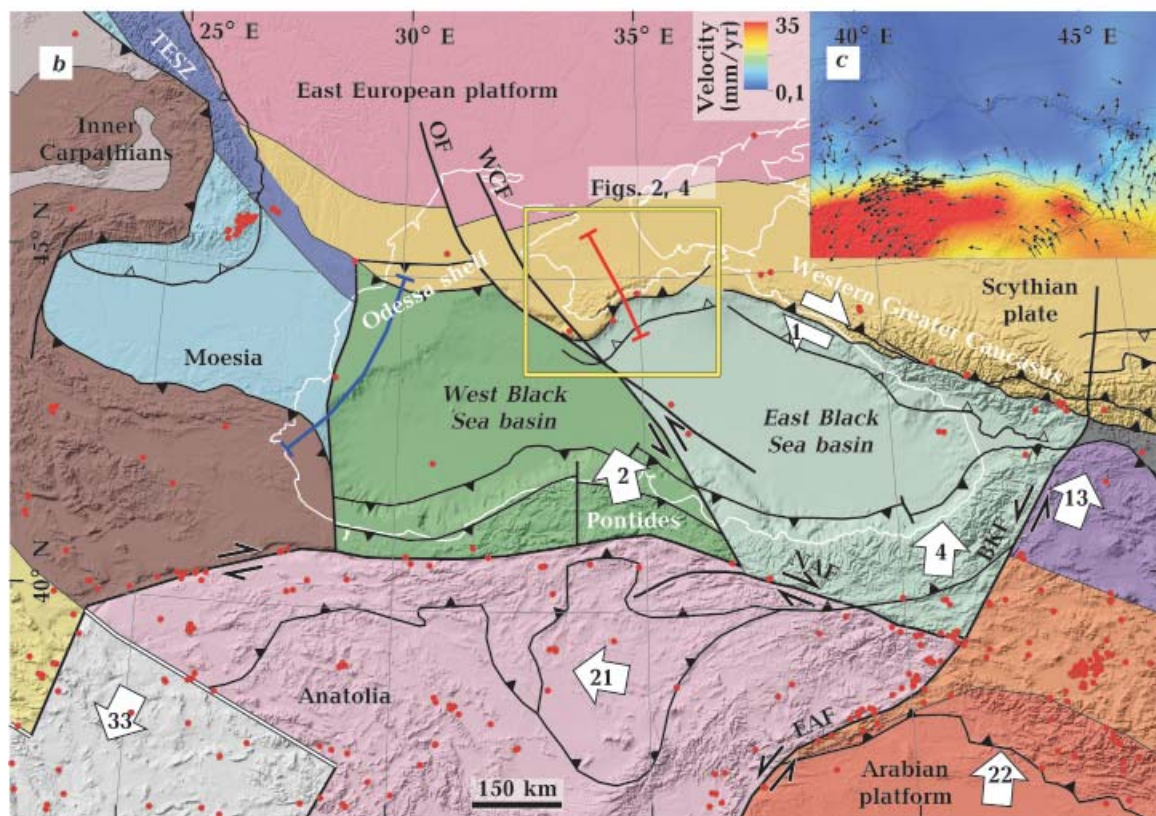
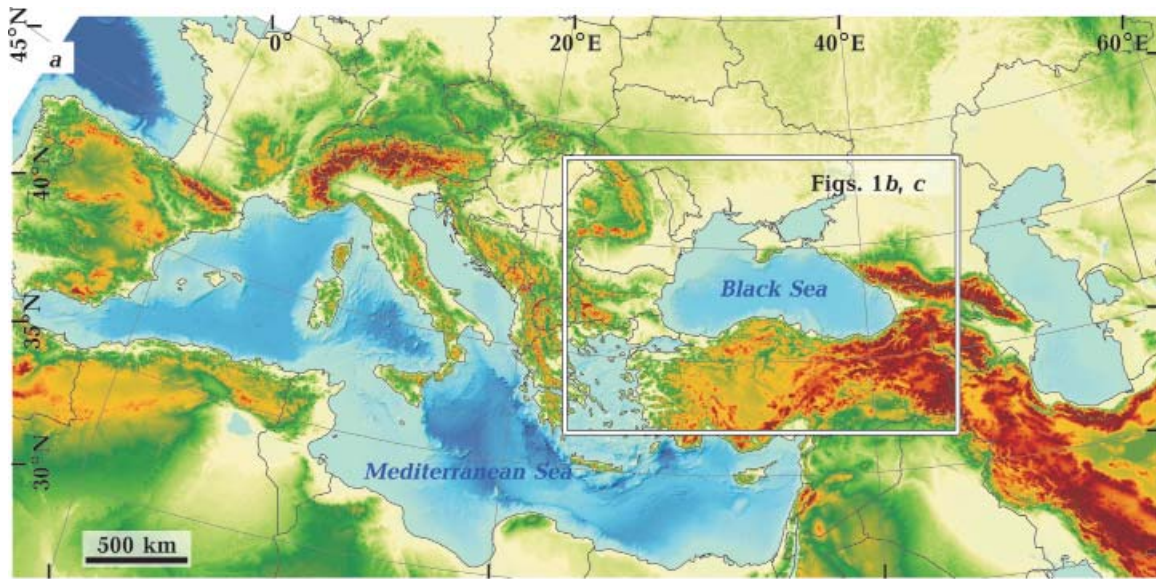


Fig. 1. Location of Arabia-Eurasia collision zone within the Alpine-Himalaya belt (a). Tectonic map of the Black-Sea basin and adjacent areas modified from [Reilinger et al., 2006; Schmid et al., 2008; Munteanu et al., 2013; Nikishin et al., 2015a, b; Sheremet et al., 2016a, b] (b). Blue line — balanced cross section location from [Munteanu et al., 2013]; red dots — earthquake epicenters ($M > 4.5$; USGS earthquake catalogue 2000 to 2016); thrusts with filled and open triangles — thick- and thin-skinned thrusts; double line — extensional plate boundary; plain lines — strike-slip faults; white arrows and corresponding numbers — GPS-derived plate velocities (mm/yr) relative to Eurasia [Reilinger et al., 2006]; NAF — North Anatolian fault; EAF — East Anatolian fault; OF — Odessa fault; WCF — Western Crimean fault; TESZ — Trans-European Suture Zone. Map showing GPS velocity and movement direction of the Black Sea and neighboring areas relative to Eurasia (modified from [Reilinger et al., 2006]) (c).

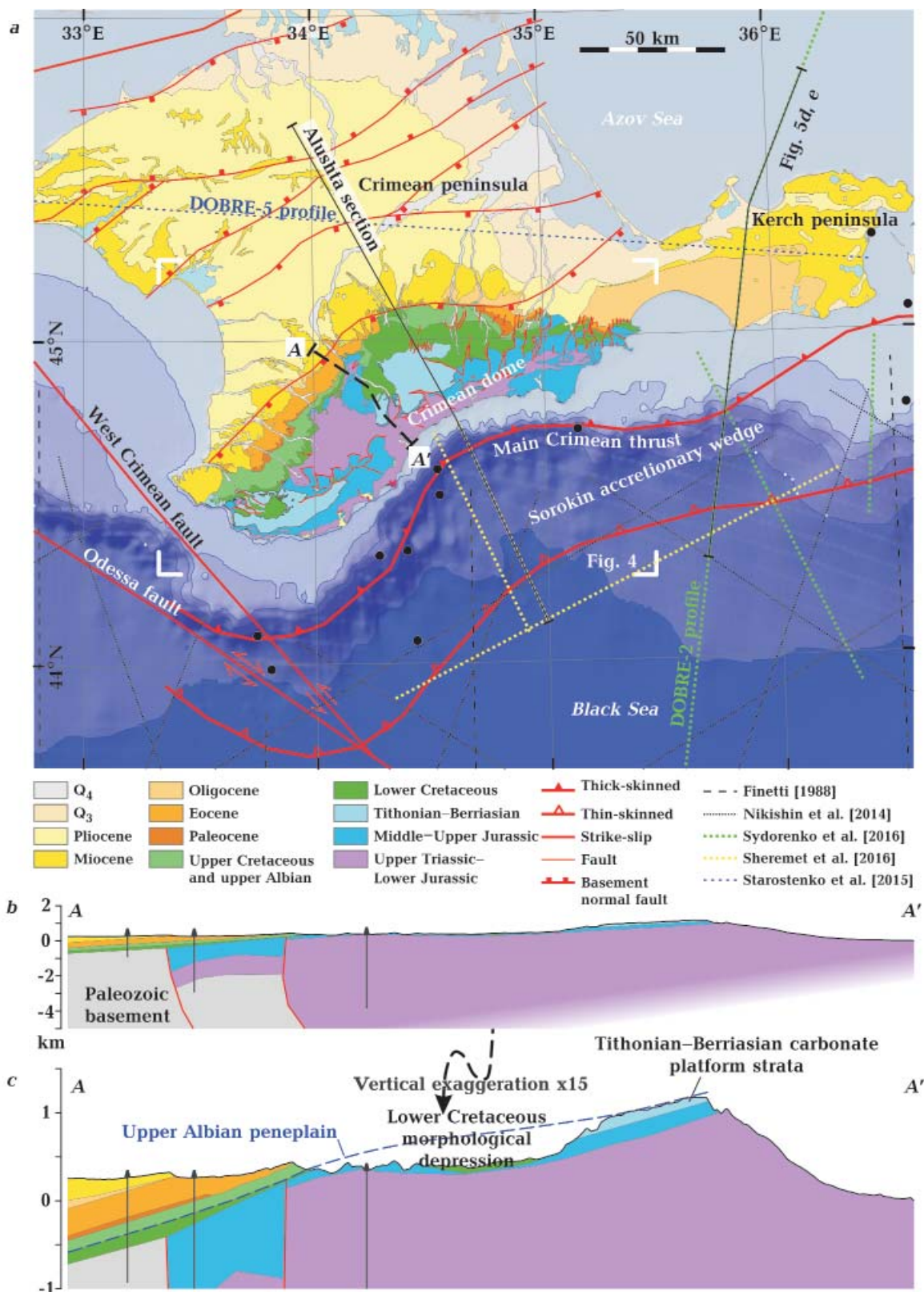


Fig. 2. Geological map of the Crimean thrust-fold-belt (a) and geological section across the Crimean dome along line A—A' modified from [Muratov, Sydorenko, 1969] (b). Wells are projected into the line of section. Basement normal faults are taken from [Tchaikovsky et al., 2006]. Vertically exaggerated upper part of the A—A' cross section line (c). Black line in a traces the balanced cross section; black dots, earthquake epicenters $M_L=4\div 5$ (after [Yegorova, Gobarenko, 2010]).

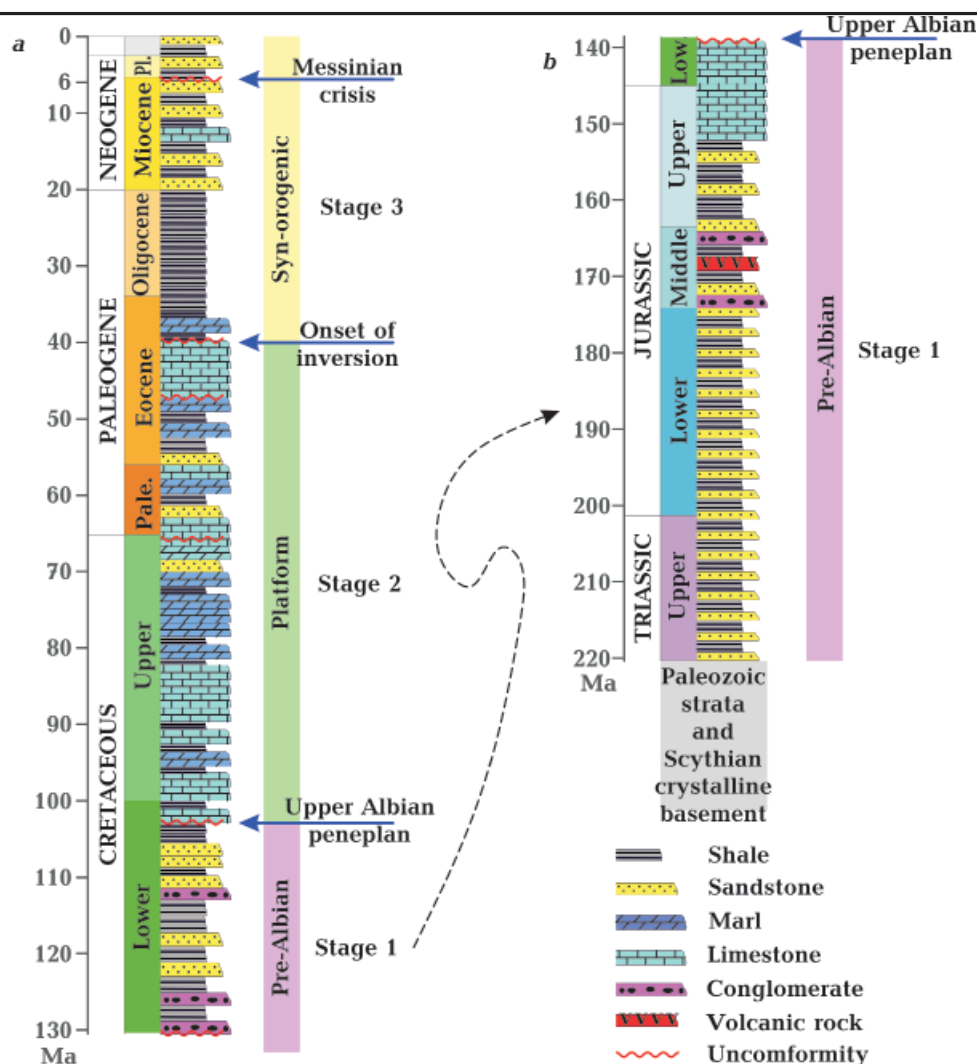


Fig. 3. Simplified stratigraphy along the A—A' geological cross section (see Fig. 2 for location). The northern slope of the Crimean dome modified from [Nikishin et al., 2015a] (a) and the crest of the Crimean dome modified from [Muratov, Sydorenko, 1969] with the three major stages of Mesozoic—Cenozoic basin evolution (b); see text for details. The erosional surface of the Messinian crisis relates to offshore data.

line basement of the Scythian plate and its deformed and partly eroded Triassic—Lower Cretaceous cover. 2. The Upper Albian—Middle Eocene sequence records the build-up of a platform on a passive continental margin. 3. The Middle Eocene—Recent strata comprise a syn-orogenic sedimentary rock sequence. According to the DOBRE regional seismic profiles (see Fig. 2, a), the crust below the Crimean peninsula is 40—50 km thick and gradually thins southward [Yegorova, Gobarrenko, 2010; Starostenko et al., 2015, 2016]. The Scythian crystalline basement was drilled to 0,2—2,0 km depth [Muratov, 1960]; the

hanging Paleozoic sedimentary rocks — also only known from wells — are 1—5 km thick [Muratov, Sydrenko, 1969]. Upper Triassic to Lower?Middle Jurassic and Lower Cretaceous flysch and intervening Middle Jurassic volcanic rocks and Tithonian—Berriasian carbonate platform strata — the latter up to 1,2 km thick — record the complex Mesozoic passive margin evolution. The Tithonian—Berriasian limestones, more resistant than the surrounding flysch, occupy the highest elevations of the Crimean peninsula, forming relatively flat, northwest dipping slopes; the limestones are capped by a locally preserved

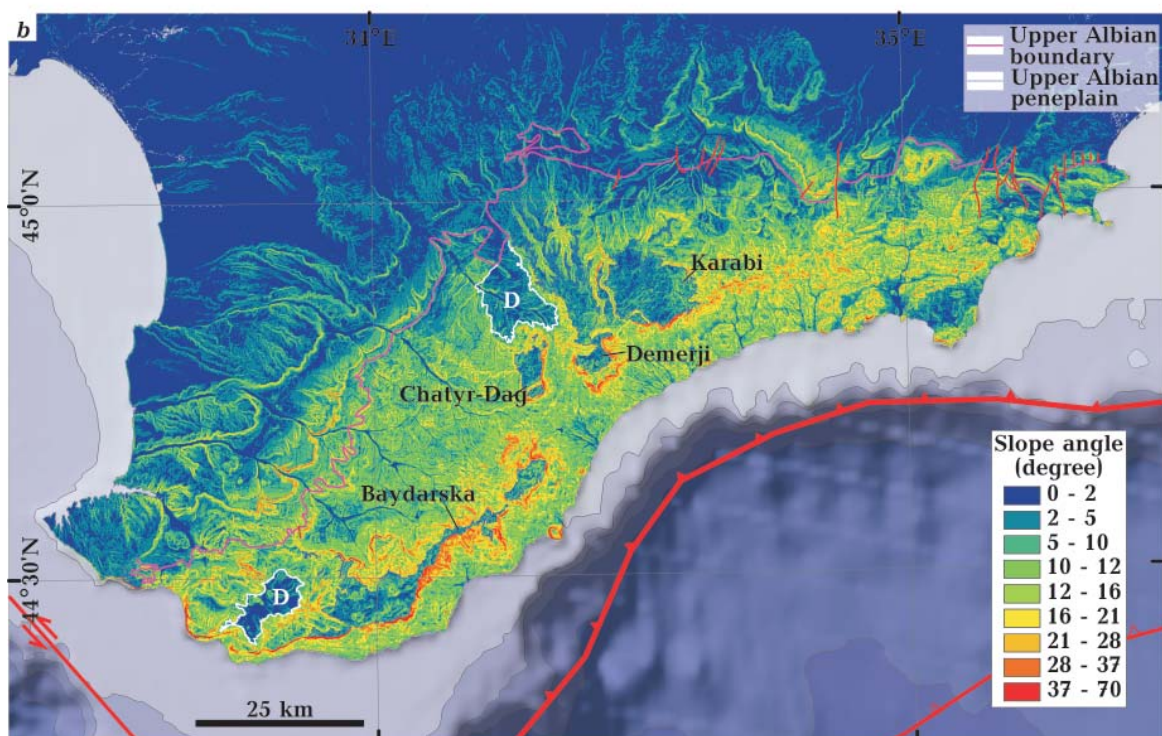
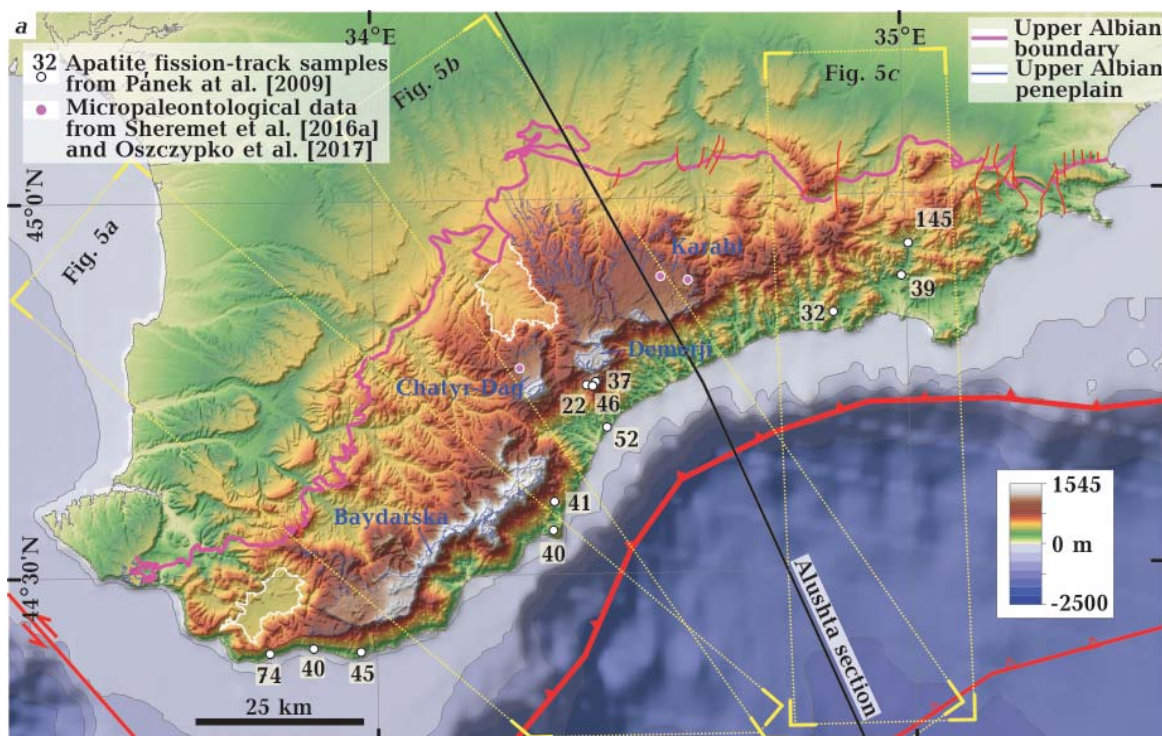


Fig. 4. Shaded relief map (a) and slope-gradient map of the southern Crimean peninsula and the northern Black Sea and the position of the swath profiles (b) (yellow frames) shown in Fig. 5. Purple line marks the outcrop trace of the peneplain, i. e., the boundary between pre-Albian flysch and the Upper Albian—Middle Eocene platform strata. Blue lines outline the upper Albian peneplain relicts within the mountains of the southern peninsula. White lines frame morphological depressions not related to the peneplain.

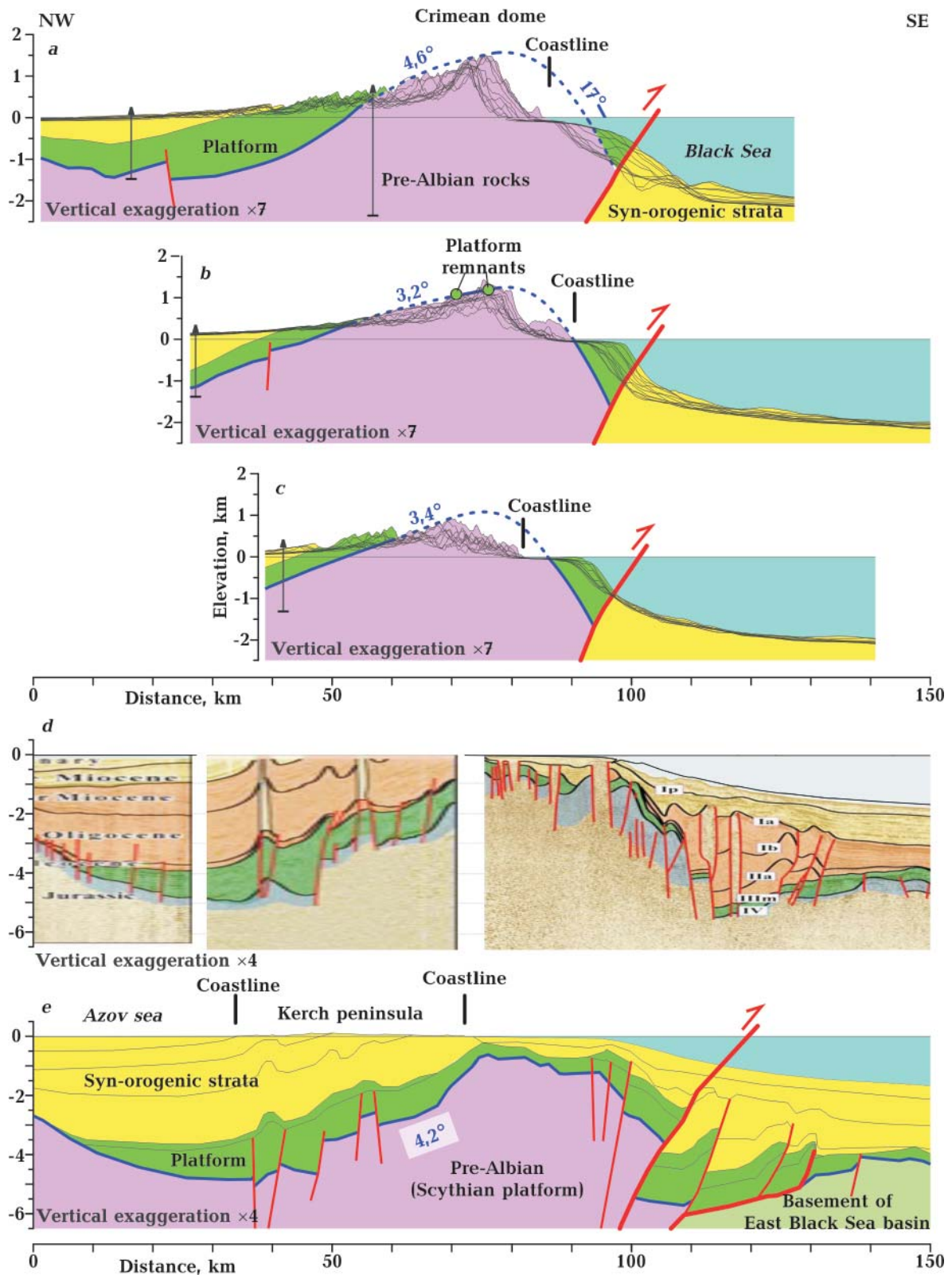


Fig. 5. A series of 20–25 km wide, strike-normal topographic swath profiles across the Crimean fold-thrust belt from west (a) to east (c). Location profiles see Fig. 4, a. Gray lines show mean surface slope. The dotted blue line traces the highest elevations, interpreted to represent a little eroded upper Albian peneplain. The strike of the continental slope is a bit oblique to the westernmost profile, slightly shifting the slope lines offshore in a. The peneplain connects with the exposure traces of the basal strata of the platform deposits north and south of the

upper Albian erosional surface (see below [Pánek et al., 2009] (Fig. 2, *b, c*). The Upper Cretaceous—Eocene deposits (stage 2) cover the Triassic—Lower Cretaceous strata unconformably. The northern slope of the Crimean dome and the hinterland of the Crimean fold-thrust belt (north of the dome) preserve a continuous section of these platform deposits; their thickness varies from 0,3 to 8,0 km [Muratov, Sydorenko, 1969; Tchaikovsky et al., 2006; Sheremet et al., 2016b]. The platform sedimentation terminated in the middle Eocene due to uplift induced by the underthrusting of the East Black-Sea basin lithosphere below the Scythian plate [Nikishin et al., 2001; Pánek et al., 2009]. A middle Eocene angular unconformity at the base of the synorogenic deposits (stage 3) records the onset of shortening; middle Eocene massive nummulitic limestones unconformably cover the older rocks [Muratov, 1960; Lysenko, Janin, 1979; Afanasenkov et al., 2007; Sheremet et al., 2016a]. The Oligocene—Miocene strata consist of up to 2 km thick grey, and brownish to reddish clays (Maykop Formation) and unconformably overlie the middle Eocene limestone [Nikishin et al., 2015c; Sheremet et al., 2016a]. The Neogene consists mostly of shallow marine terrigenous-carbonate deposits. In Sorokin accretionary wedge, seismic reflection data record syn-tectonic growth strata from the Middle Oligocene to the Middle Pliocene [Sheremet et al., 2016b]. Offshore, a sharp disconformity, visible in the seismic sections, traces a major erosional surface; it is interpreted to record the Messinian crisis (~6—5 Ma), resulting from an important sea level drop [Krijgsman et al., 2010; Sheremet et al., 2016b].

Geomorphological analysis. We combined the 90 m resolution Shuttle Radar Topography Mission data with the bathymetric data for the Black Sea from the 30 arc sec General Bathy-

metric Chart of the Oceans to construct relief and slope-gradient maps and three swath profiles, normal to the strike of the Crimean fold-thrust belt structures (Figs. 4, 5). The area with a slope $<5^\circ$ constitutes a paleo-surface or plateau that corresponds to the upper Albian unconformity between the Triassic—Lower Cretaceous and the Upper Albian—Middle Eocene rocks; it represents a large and flat erosion surface or peneplain [Pánek et al., 2009]. Two relatively flat surfaces — west of Baydarska and north of Chatyr-Dag plateaus — are Lower Cretaceous erosional depressions, significantly lower than the Upper Albian peneplain (see Fig. 2, *c*; the depressions are marked with «D» in Fig. 4, *a*).

We traced the paleo-surface regionally by connecting the highest elevations along the swath profiles, interpreting them to have experienced little erosion into the Tithonian—Berriasian platform carbonates below the peneplain (Fig. 2, 5, *a—c*). A few remnants of Upper Cretaceous strata — dated micropaleontologically — outline the paleo-surface at the highest elevations in the Chatyr-Dag and Karabi areas (Fig. 4, *a*) [Sheremet et al., 2016a; Oszczypko et al., 2017]. North of Demerji (see Fig. 4), Upper Albian—Middle Eocene platform rocks overlie the peneplain directly. Erosion destroyed the paleo-surface along the southern coast of the Crimean dome, but the Upper Albian—Middle Eocene platform rocks north of the Main Crimean thrust are preserved offshore; there, they dip $\sim 17^\circ$ southeast (see Fig. 5, *a, c*) [Sheremet et al., 2016b]. We traced the peneplain across the Crimean dome, connecting the upper Albian unconformity mapped onshore with its offshore parts (blue lines in Fig. 5, *a, c*). We infer that the northwest and southwest dips of this paleo-surface determine the backlimb and forelimb geometries, respectively, of the large-scale antiform that constitutes the Crimean

Crimean dome. The dips of the peneplain ($3,2—4,6^\circ$ without vertical exaggeration) outline the large-scale antiform of the Crimean dome. Fragments of the seismic profile of [Sydorenko et al., 2016] (*d*), which location is shown in Fig. 2, *a*, and cross section reinterpreting *d* (*e*). Pink, green, and yellow colored rock packages highlight the three main stages of the stratigraphic evolution, i.e., the pre-Albian rocks below the Upper Albian peneplain, the Upper Albian to Middle Eocene platform deposits, and the post Middle Eocene syn-orogenic deposits. Blue line, position of the Upper Albian peneplain (see Fig. 3).

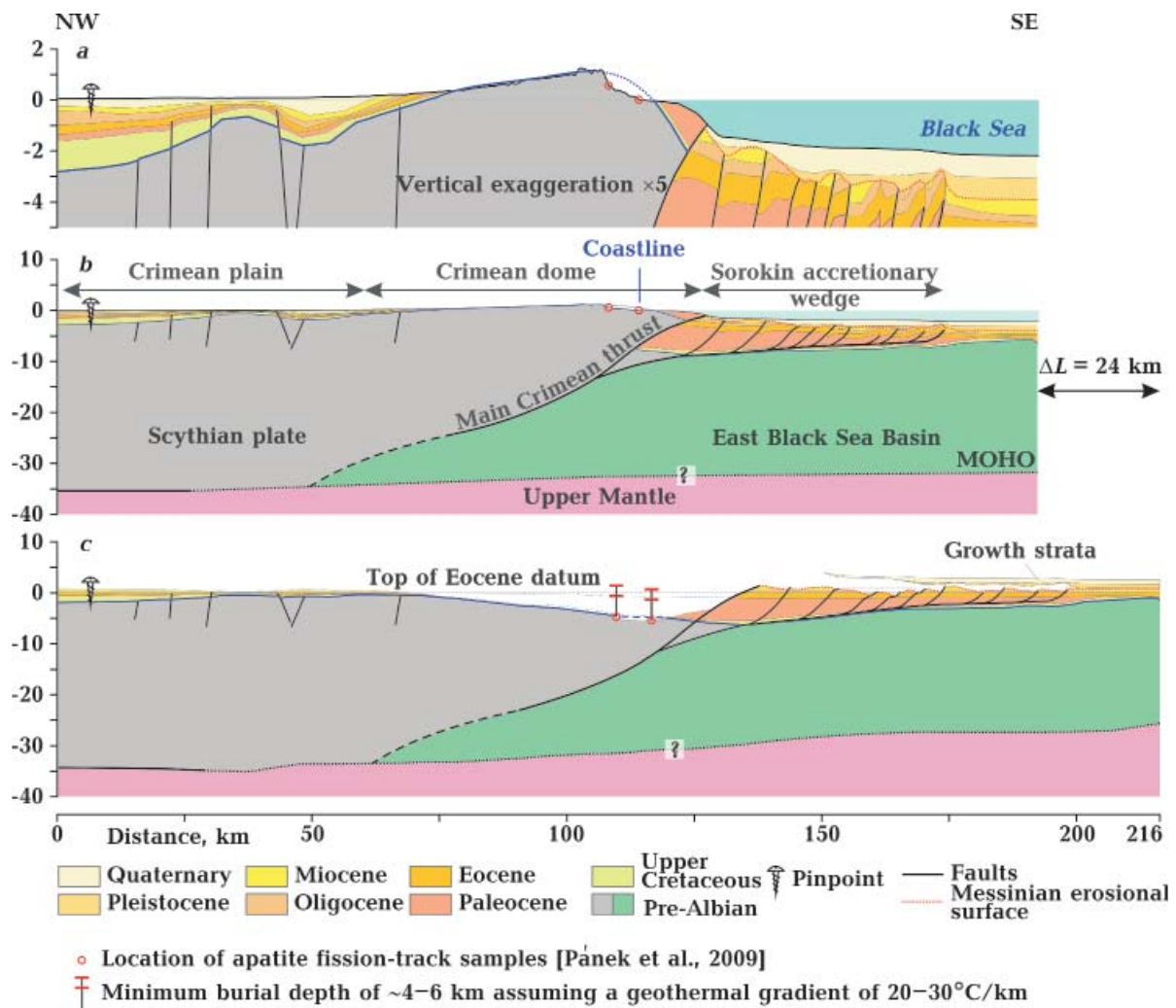


Fig. 6. Vertically exaggerated upper part of the Alushta balanced cross section (a), balanced (b) and restored (c) Alushta cross section. Fig. 2 for location. ΔL — total shortening.

dome; the dome formed as a thick-skinned structure above the Main Crimean thrust (see Fig. 5, a, c). The dip of the forelimb above the Main Crimean thrust approximately determines the continental slope in the Black Sea (see Fig. 2, 5). Farther east, across the Kerch peninsula, the DOBRE-2 seismic line reveals a map-scale antiformal structure — the Crimean dome — and a part of the leading Sorokin accretionary wedge [Sydorenko et al., 2016] (see Fig. 2, 5, d, e). The oblique orientation of this seismic line to the tectonic transport direction precludes the construction of a balanced cross section. An estimate of the total shortening along the section yielded at least 12 km, less than across the Crimean peninsula

and its offshore part (see below). This is line with the less deep erosion across the Kerch peninsula than across the Crimean peninsula; this allowed the preservation of the upper Albian peneplain and the Upper Albian—Middle Eocene platform rocks.

Balancing cross section. We combined the geometry of the antiform above the Main Crimean thrust with the geometry of the Sorokin accretionary wedge outlined by the offshore seismic data [Sheremet et al., 2016b; Sydorenko et al., 2016]. Together with the available low-temperature thermochronologic ages [Pánek et al., 2009], these data constrain the present geometry and the structural evolution of the Crimean fold-and-thrust

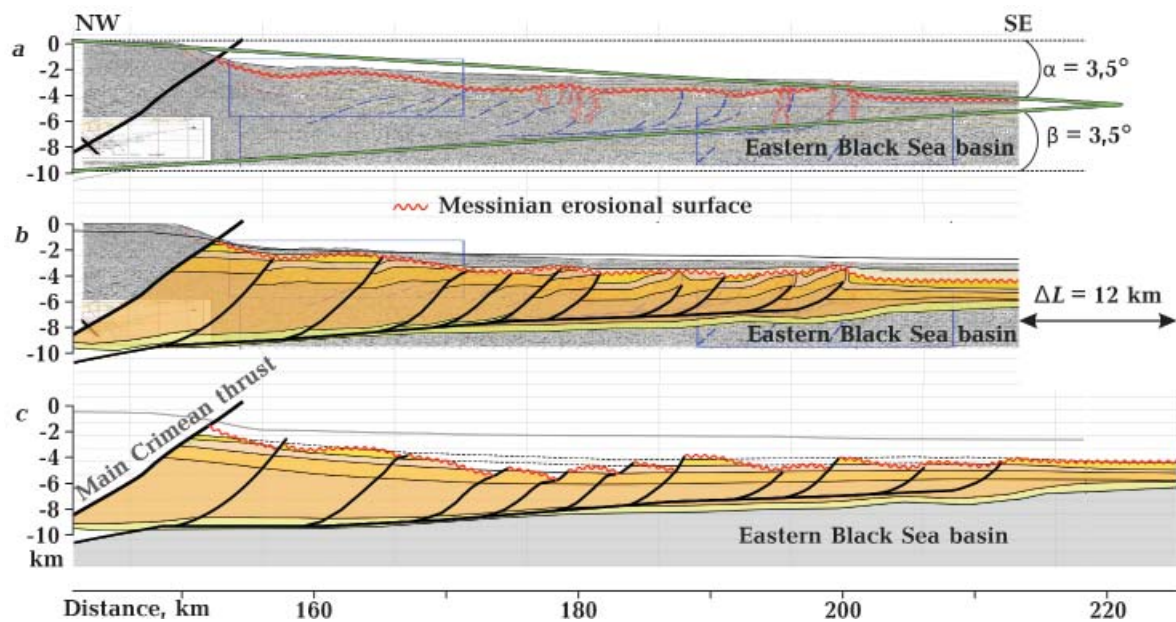


Fig. 7. Offshore seismic line of [Sheremet et al., 2016b] across the Sorokin accretionary wedge (a). Green lines outline the critical cohesive Coulomb wedge, defined by a $3,5^\circ$ surface slope (α) and a $3,5^\circ$ dip of the basal detachment (β). Table for calculation parameters. Balanced and c restored cross sections of the Sorokin accretionary wedge (b). The wedge is interpreted as a series of splay faults bounding post-Albian platform and syn-orogenic rocks above a basal detachment. Fig. 6 for legend. ΔL — total shortening.

belt. We used cross-section balancing and forward modeling. The Alushta cross section extends 192 km NW—SE from the middle of the Crimean peninsula at $45^\circ 40' N$, $33^\circ 55' E$, through the remnants of the peneplain at Karabi, to $44^\circ 07' N$, $34^\circ 59' E$ in the Black Sea (Fig. 2, 4, 6, a, b); this section nearly coincides with the one of [Sheremet et al., 2016b].

Detailed geological maps based on abundant exposures constrain the Crimean fold-thrust belt north of the Crimean dome (e. g. [Muratov, Sydorenko, 1969; Tchaikovsky et al., 2006]). Its southern part occupies the submarine Black-Sea shelf, continental rise, and abyssal plain. Our interpretations follow those given by [Robinson et al., 1996, Starostenko et al., 2016, Vakarchuk et al., 2016], which use the structures visible in the reflection seismic lines (see Fig. 2) [Finetti, 1988; Nikishin et al., 2015a, b; Sheremet et al., 2016b; Sydorenko et al., 2016]. The major structural features of the Alushta section (Fig. 6, a, b) are from north to south the Crimean platform and the Crimean dome, which exposes the pre-Albian sequence. To the south — under the abyssal plain — the Sorokin accretionary wedge

comprises a thin-skinned belt above a basal detachment (Fig. 6, 7).

Construction of the balanced cross section. Our balanced cross-section construction used a few general assumptions: throughout the deformation history, line length and surface area remain constant; a common basal detachment underlies both the Crimean dome and the Sorokin accretionary wedge; the structural geometry can be modeled with the fault-parallel-flow and trishear algorithms; the preferred restorations requires a minimum of shortening and explains the geological data. We interpret the internal structure of the Sorokin accretionary wedge as a series of splay faults, shortening the post-Albian platform and syn-orogenic strata above a basal detachment (see Fig. 7); the construction used fault-parallel flow mechanism. In its frontal part, individual folds can be traced in the seismic line. Their geometries — dips and thickness of the strata increase smoothly and incrementally from anticlinal crest to the limbs — suggest shortening by trishear fault-propagation folding (e. g. [Erslav, 1991; Hardy, Ford 1997]). The dip and depth

Measured and inferred parameters of the Sorokin accretionary wedge

Detachment depth, m	H	6500	9000	Given by the balanced cross sections
Local depth, m	D	2000	100	Given by the general bathymetric chart
Overall surface slope in degrees	α	3,5		Given by the balanced cross sections
Regional detachment dip, degrees	β	3,5		$\beta=(5,9^\circ-\alpha)/0,66$ from [Davis et al., 1983]
Internal coefficient of friction	μ	0,9—1,0		From [Dahlen et al., 1984]
Basal coefficient of friction	μ_b	0,85		Assumed; based on laboratory measurements of maximum friction of many silicate rocks [Byerlee, 1978]
Fluid-pressure ratio	λ	0,9		From [Davis et al., 1983]
Basal fluid-pressure ratio	λ_b	0,9		From [Davis et al., 1983]
Density of water, kg/m ³	ρ_w	1000		—
Mean density, kg/m ³	ρ	2500		From [Dahlen et al., 1984]
Acceleration of gravity, m/s ²	g	9,8		—
Coefficient of dependency basal coefficient of friction to accretionary wedges parameters	K	5,3		$K = \frac{\tan^{-1} \mu_b + \beta}{\alpha + \beta}$
Vertical normal traction, MPa	σ_z	178,9	240,1	$\sigma_z = \rho_w g D + \rho g H$
Pore fluid pressure, MPa	P_f	162,9	216,2	$P_f = \lambda \times (\sigma_z - \rho_w g D) + \rho_w g D$
Basal shear traction, MPa	τ_b	418,3	579,2	$\tau_b = ((\alpha + \beta) \times (1 - \rho_w / \rho) + (1 - \lambda_b) K) - (1 - \rho_w / \rho) \beta \times \rho g H$

of the basal detachment in the frontal part of accretionary wedge is taken from the seismic reflection data (Fig. 7, *a*). We postulate that the penepplain at the top of the pre-Albian sequence acted as this detachment over most to the wedge's north—south extent; in the southeast, at the wedge front, it climbed into Paleocene deposits. In addition, we used the critical Coulomb-wedge model of Davis et al. [1983] and Dahlen et al. [1984] to calculate the dip angle of the detachment. First, the swath profiles across the wedge define its surface slope at $\sim 3,5^\circ$. Assuming a critical state and a rheology typical for sedimentary wedges (Table), we calculated a $3,5^\circ$ dip for the base of the wedge, comparable with that

estimated from the seismic data. The in this way estimated depth to the basal detachment of the Sorokin accretionary wedge is $\sim 6,5$ km beneath the frontal part, ~ 9 km in the middle (see Fig. 7), and ~ 15 km below the frontal part of the Crimean dome (see Fig. 6). This is deeper than suggested by [Sheremet et al., 2016b], who used a depth of $6,0$ — $6,5$ km for the entire wedge. Using the critical wedge model, we also calculated the basic traction, created by the subduction of the East Black-Sea microplate beneath the Scythian plate. The results are presented for two points at $6,5$ and $9,0$ km depth along the detachment. The values are at best approximate due to the uncertain input parameters; nevertheless, they

represent a maximum possible fluid pressure, important for and testable by future drilling.

We modeled the Crimean dome as a fault-ramp fold above the Main Crimean thrust as

the basal detachment (see Fig. 6). The preserved parts of the upper Albian peneplain determine the geometry of the back- and forelimbs; the backlimb dips $\sim 4^\circ$ NW, the forelimb

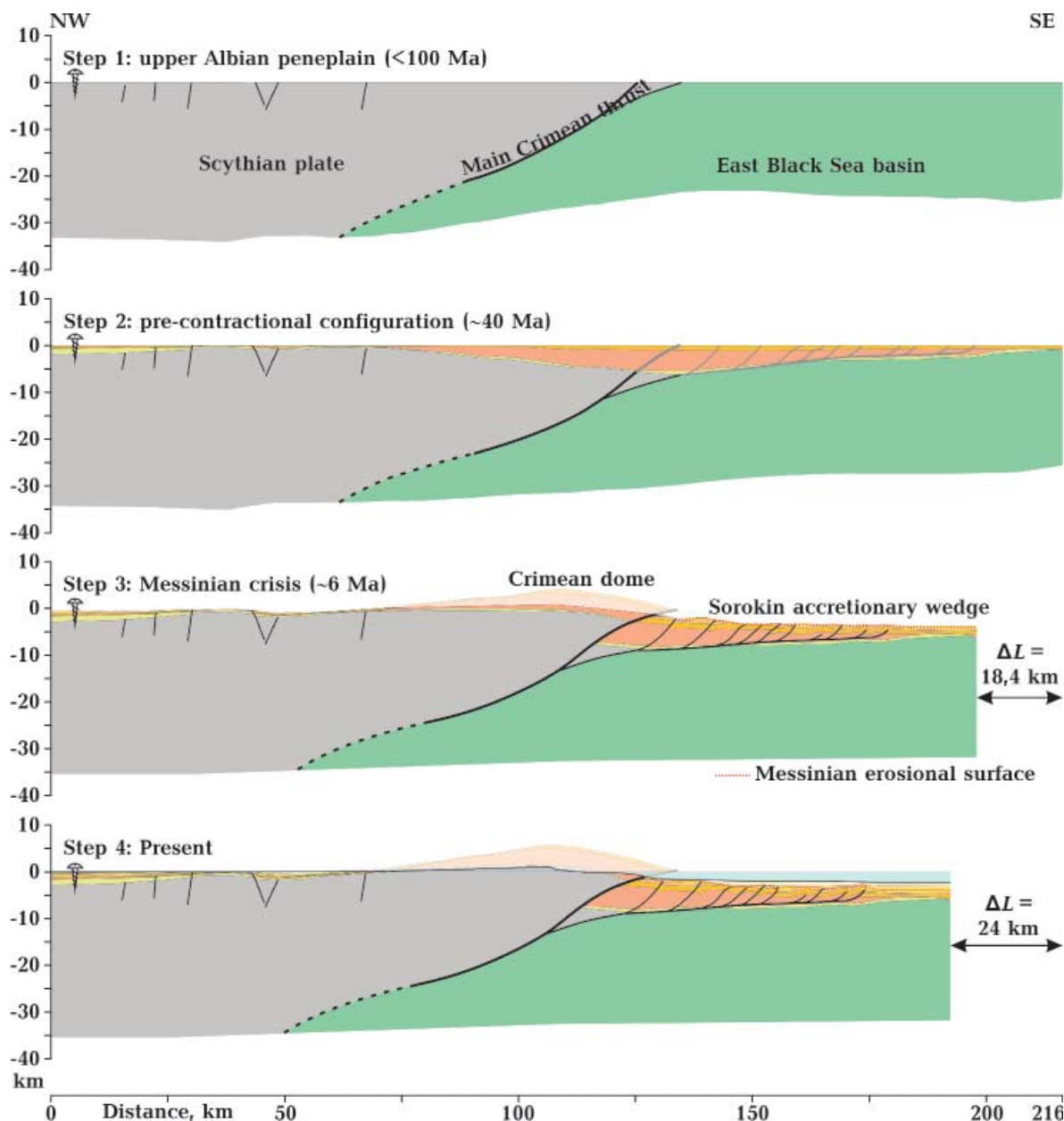


Fig. 8. Four steps of the forward model showing the kinematic evolution of the Crimean fold-and-thrust belt based on cross-section balancing, apatite fission-track [Pánek et al., 2009], and stratigraphic data [Nikishin et al., 2015c; Sheremet et al., 2016a]. Step 1 shows the vast peneplain along the boundary between the pre-Albian rocks (crystalline basement of the Scythian plate and its deformed and differentially eroded Triassic—Lower Cretaceous cover) and the Upper Albian to Middle Eocene platform sequence. Step 2 shows the undeformed Lower Cretaceous—Middle Eocene platform deposits with their variable (0,3—8,0 km) thickness. The onset of inversion at ~ 50 —32 Ma (~ 40 Ma) is dated by apatite fission-track thermochronology and growth strata within the backlimb of the Crimean dome and in the Sorokin accretionary wedge. Step 3 shows the major structural geometry completed. The flat Messinian erosional surface, marking a sea level drop, allows the post-Messinian restoration of the frontal part of the fold-thrust belt. Steps 4 shows the present-day geometry. For legend, see Fig. 6. See text for details.

~17° SE (see Fig. 5, *a—c*). The depth to the basal detachment under the Crimean dome is the fundamental parameter that controls the deformation geometry. We assumed that the Main Crimean thrust reactivated a normal fault between of the Scythian plate and the Eastern Black-Sea basin that formed during the Triassic—Jurassic active continental margin construction [Nikishin et al., 2015c]. Northeast trending, large basement normal faults within the Crimean peninsula were mapped by drilling and seismic data [Tchaidkovsky et al., 2006] (see Fig. 2). Most of these faults dip ~50—70° NW and have a vertical offset of hundreds to thousands of meters. By trial-and-error, we approximated a solution that fits the geometry of the Crimean dome; the best-fit model for the Alushta section (see Fig. 6, *b*) has a 30° dip for the Main Crimean thrust, which caused ~12 km of thick-skinned shortening in its hanging wall.

Restored cross section. Fig. 6 shows deformed and restored line lengths for the Alushta section; the pinpoint is in the hinterland on the Scythian platform. We used the top of the Eocene datum as the reference horizon for the calculation of the total shortening over the entire length of the sections. We obtained ~24 km of shortening on this horizon. The thin-skinned Sorokin accretionary wedge and the thick-skinned Crimean dome each yielded ~12 km of shortening. The total value, ~24 km, is higher than the one obtained by [Munteanu et al., 2011] for the northern Western Black-Sea basin (see blue section line in Fig. 1, *b*); they estimated ~16 km of shortening during the late Middle Eocene—Pliocene.

Solov'ev and Rogov's [2009] detrital zircon fission-track data from the pre-Albian terrigenous complexes of the Crimean dome yielded ages ≥ 154 Ma. Therefore, the Cenozoic burial did not heat these rocks above the effective fission-track annealing temperature of 240 ± 30 °C of natural zircon [Hurford, 1998]; assuming a geothermal gradient of 20—30 °C/km, these rocks experienced <7,5—10,0 km of burial. Fig. 4, *a* shows the location and ages of the apatite fission-track samples of Pánek et al. [2009] along the southern coast of the Crimean peninsula. Most of the ages cluster

in the Eocene (~50—32 Ma, median=41 Ma); the westernmost sample yielded an Upper Cretaceous age (~74 Ma), the easternmost one a Jurassic—Cretaceous age (~145 Ma). Along the Alushta section, all sample were reset in the Eocene—Oligocene; this translates into a 4—6 km thick, eroded overburden above the restored position of each sample using an apatite fission-track closing temperature of ~120 °C, and, again, a geothermal gradient range of 20—30 °C/km. We projected the positions of the northern and southern sample groups (see Fig. 4, *a*) onto the Alushta section with their positions restored according to the structural model (see Fig. 6, *b, c*). These restorations — shown as red bars above the erosional profile in the restored cross section (see Fig. 6, *c*) — give the minimum thickness (~4—6 km) of the stratigraphic column prior to erosion. The top of this pre-erosional stratigraphic column corresponds to the upper Eocene. The onset of erosion then cooled the samples through the apatite fission-track closure temperature, indicating that shortening occurred in the Eocene—Oligocene.

Discussion. To visualize the structural evolution of the Crimean fold-thrust belt, Fig. 8 shows a kinematic forward model based on the balanced cross section. This model accounts for the dimensions of individual structures, their growth succession, the offsets along the thrusts, and the modeling algorithms that are best suitable to describe the observed structural geometries (fault-parallel flow and trishear). In the following, we describe four steps of the kinematic evolution.

Step 1: Upper Albian peneplain at <100 Ma. The peneplain is defined by the boundary between the deformed and differentially eroded Triassic—Lower Cretaceous cover above the crystalline basement of the Scythian plate and the Upper Albian—Middle Eocene carbonate platform rocks (see Fig. 2). The Upper Albian and younger formations (stage 2 strata in Fig. 3) are transgressive on the pre-Albian rocks (stage 1 strata in Fig. 3) and form an almost continuous sedimentary cover. The position of the Main Crimean thrust may be inherited from the Triassic—Lower Cretaceous continental margin extension and is probably

a reactivated low-angle normal fault. As most of the mapped and imaged normal faults are steeper, such a normal fault must have had a listric geometry at depth or was rotated to a shallower dip during passive margin formation.

Step 2: pre-contractual configuration at ~40 Ma. Inversion affected undeformed Upper Cretaceous—Middle Eocene platform deposits with a thickness varying between 0,3 and 8,0 km. The apatite fission-track thermochronology, the stratigraphy in the Crimean dome, and the growth strata in the Sorokin accretionary wedge time the onset of inversion. Pánek et al. [2009] dated shortening-related erosion in the Crimean thrust-fold belt as Middle Eocene—Lower Oligocene and the deposition of syn-orogenic strata during the Oligocene—Lower Miocene (Maikopian) times this Cenozoic deformation offshore: clays and siltstones form up to 2 km thick, flysch-like strata [Nikishin et al., 2015c].

Step 3: Messinian crisis at ~6 Ma. The Messinian erosion surface, a result of an important sea level drop [Sheremet et al., 2016b], developed sub-horizontally. It provides an offshore datum for the estimation of the pre- and post-Messinian shortening (Fig. 6, steps 3 and 4). The pre-Messinian shortening across the Sorokin accretionary wedge was ~9,2 km, implying that the major structural geometry was completed before the Messinian erosion surface developed. The post-Messinian shortening amounted to ~2,8 km. Whereas the pre-Messinian shortening likely occurred mostly by in-sequence thrusting, the faulting and folding of the Messinian erosion surface at several locations in the Sorokin accretionary wedge (see Fig. 4, 7a of [Sheremet et al., 2016b] for details) imply out-of-sequence reactivation along blind thrusts.

Our balancing showed that the total amount of shortening above the Main Crimean thrust is ~12 km. The restriction of the Messinian erosion surface to the offshore part of the cross section does not allow a subdivision into pre- and post-Messinian stages for the Crimean dome. Earthquake with a magnitude of $M_L=4\div 5$ with focal depths of 20—30 km along the Main Crimean thrust, indicating NW—SE compression (see Fig. 2)

[Smolyaninova et al., 1996], and ongoing slow cooling of rocks in the Crimean dome [Pánek et al., 2009] suggest that the Main Crimean thrust is still active; it may have been active continuously. We therefore speculate that the Main Crimean thrust was active with the same shortening rate as the Sorokin accretionary wedge during post-Messinian times. The total pre-Messinian shortening would then be ~18,4 km, the post-Messinian one ~5,6 km.

Steps 4: present-day geometry. The model implies minimum shortening. Since the onset of deformation at 50—32 Ma (median=41 Ma [Pánek et al., 2009]), ~4—6 km of overburden has been eroded from the crest of Crimean dome with an average shortening rate between the Scythian platform and the Eastern Black-Sea basin of ~0,6 km/Ma (~24 km over ~40 Ma). Since the Messinian crisis at 6,0—5,3 Ma, ~5,6 km of shortening may have occurred; if true, this would imply an increase of the convergent rate to ~0,9—1,0 km/Ma. The latter corresponds to the right-lateral slip rates of 0,6—1,3 km/Ma along the boundary between the Eastern Black-Sea basin and the Western Great Caucasus deduced from the block model [Reilinger et al., 2006]; this rate must have been accommodated across the Crimean fold-thrust belt. In addition, enhanced uplift has taken place in the Western Greater Caucasus since ~5 Ma [Avdeev, Niemi, 2011], possibly synchronously with the acceleration of shortening in the Crimean fold-thrust belt.

Conclusions. Geomorphological analysis of relief and slope across the fold-thrust belt of the southern Crimean peninsula outlines a regionally traceable surface that is interpreted to correspond to an upper Albian unconformity between Triassic—Lower Cretaceous flysch and carbonate rocks and upper Albian to middle Eocene platform rocks; it represents a large and flat erosion surface or peneplain. We infer that the northwest and southeast dips of this paleo-surface determine the backlimb and forelimb geometries, respectively, of a large-scale antiform — the Crimean dome. This dome formed as a thick-skinned structure above the Main Crimean thrust.

A new balanced cross section across the Crimean fold-thrust belt uses known outcrops relations in the onshore Crimean dome, geomorphological analysis to constrain the geometry of the dome's antiform, seismic reflection data of the offshore section under the northern Black-Sea basin, and structural interpretations that result in conservative shortening estimates. The section implies a basal detachment that deepens from ~6 km depth below the offshore accretionary wedge in the south to >30 km depth beneath Crimean dome in the north. About 24 km of shortening occurred

across the central part of the Crimean fold-thrust belt, which also shows the deepest erosion and highest surface uplift. Thick-skinned shortening in the Crimean fold-thrust belt started in the middle Eocene–lower Oligocene (~50–32 Ma) and propagated southeastward into the Black Sea, forming the thin-skinned Sorokin accretionary wedge.

Acknowledgments. We thank Midland Valley's Academic Software Initiative for access to the Move Software package. DAAD and the State of Saxony funded M.N.'s research at the TU Bergakademie Freiberg.

Geometry and Cenozoic evolution of the Crimean fold-thrust belt from cross-section balancing and kinematic forward modeling

© M. Nakapelyukh^{1, 2}, V. Belskyi³, L. Ratschbacher, 2018

The Crimean fold-thrust belt comprises the onshore Crimean-dome fold-thrust belt and the offshore Sorokin accretionary wedge, a sub-surface imbricate stack with high oil and gas potential. We combine geomorphological and balanced cross-section analyses with published low-temperature thermo-chronology and offshore seismic data to constrain both its present geometry and Cenozoic structural evolution. We interpret the Crimean dome as a map-scale, ramp-related antiform above the Main Crimean thrust, the basal detachment to the onshore part of the fold-thrust belt. The Main Crimean thrust separates the continental Scythian plate from the transitional to oceanic Eastern Black-Sea basin and likely reactivates an Upper Triassic–Lower Jurassic passive continental margin structure. The Crimean fold-thrust belt has accommodated ~24 km shortening since the Eocene, with ~12 km contraction each in the thick-skinned Crimean dome and the thin-skinned Sorokin accretionary wedge. The intermediate geometries in the kinematic evolution traced by the kinematic forward model are testable by future hydrocarbon exploration and thermochronologic studies.

Key words: Crimean fold-thrust belt, thick-skinned versus thin-skinned structural geometries, balanced cross section, kinematic forward model.

References

- Afanasenkov A. P., Nikishin A. M., Obukhov A. N., 2007. Eastern Black Sea Basin: Geological Structure and Hydrocarbon Potential. Moscow: Nauchnyy Mir, 172 p. (in Russian).
- Avdeev B., Niemi N., 2011. Rapid Pliocene exhumation of the central Greater Caucasus constrained by low-temperature thermochronometry. *Tectonics* 30, TC2009. doi: 10.1029/2010TC002808.
- Byerlee J., 1978. Friction of rocks. *Pure Appl. Geophys.* 116, 615–626.
- Dahlen F. A., Suppe J., Davis D., 1984. Mechanics of fold-and-thrust belts and accretionary wedges: Cohesive Coulomb theory. *J. Geophys. Res.* 89, 10087–10101. doi: 10.1029/JB089iB12p10087.
- Davis D., Suppe J., Dahlen F. A., 1983. Mechan-

- ics of fold-and-thrust belts and accretionary wedges. *J. Geophys. Res.* 88(B2), 1153—1172. doi: 10.1029/JB088iB02p01153.
- Erslav E., 1991. Trishear fault-propagation folding. *Geology* 19, 617—620.
- Favre E., 1877. Etude stratigraphique de la partie sud-ouest de la Crimée suivie de la description de quelques échinides de cette région par M. P. de Zeriél. Ed. H. Georg, Geneva. (in French).
- Finetti I., Bricchi G., Del Ben A., Pipan M., Xuan Z., 1988. Geophysical study of the Black Sea. *Boll. Geofis. Appl.* 30, 197—324.
- Foht K. K. (ed.), 1926. Geological map of the Crimea. 1:400000. Leningrad: Geological Committee.
- Hardy S., Ford M., 1997. Numerical modeling of trishear fault propagation folding. *Tectonics* 16(5), 841—854.
- Hurford A. J., 1998. Zeta: the Ultimate Solution to Fission-Track Analysis Calibration or Just an Interim Measure? In: *van den Haute P., de Corte F. (eds). Advances in Fission-Track Geochronology*. Solid Earth Sciences Library. Vol. 10. Springer, Dordrecht, 19—32. https://doi.org/10.1007/978-94-015-9133-1_2.
- Kazantsev Y. V., 1982. Tectonics of the Crimea. Moscow: Nauka, 112 p. (in Russian).
- Khain V. Y. 1984. Regional Geotectonics. The Alpine Mediterranean Belt. Moscow: Nedra, 334 p. (in Russian).
- Kral J., Gurbanov A., 1996. Apatite fission track data from the Great Caucasus pre-Alpine basement. *Chem. Erde* 56: 177—192.
- Krijgsman W., Stoica M., Vasiliev I., Popov V. V., 2010. Rise and fall of the Paratethys Sea during the Messinian salinity crisis. *Earth Planet. Sci. Lett.* 290(1), 183—191. doi:10.1016/j.epsl.2009.12.020.
- Kruglov S. S., Tsytko A. K. (eds.), 1988. Tectonics of Ukraine. Moscow: Nedra, 254 p. (in Russian).
- Khriachtchevskaja O., Stovba S., Stephenson R., 2010. Cretaceous-Neogene tectonic evolution of the northern margin of the Black Sea from seismic reflection data and tectonic subsidence analysis. In: *M. Sosson, N. Kaymakci, R. Stephenson, F. Bergerat, V. Starostenko (eds.). Sedimentary Basin Tectonics from the Black Sea and Caucasus to the Arabian Platform*. Geol. Soc. London Spec. Publ. 340, 137—157. doi: org/10.1144/SP340.8.
- Lysenko N. I., Janin B. T., 1979. Biostratigraphic characteristics of a typical section of the Upper Jurassic and Lower Cretaceous Central Crimea. *Proceedings of the Academy of Science of the USSR* 6, 70—80 (in Russian).
- McClusky S., Balassanian S., Barka A., Demir C., Ergintav S., Georgiev I., Gurkan O., Hamburger M., Hurst K., Kahle H., Kastens K., Kekelidze G., King R., Kotzev V., Lenk O., Mahmoud S., Mishin A., Nadariya M., Ouzounis A., Paradissis D., Peter Y., Prilepin M., Reilinger R., Sanli I., Seeger H., Tealeb A., Toksöz M. N., Veis G., 2000. Global Positioning System constraints on plate kinematics and dynamics in the eastern Mediterranean and Caucasus. *J. Geophys. Res.* 105(B3), 5695—5719. doi: 10.1029/1999JB900351
- Meijers M. J. M., Vrouwe B., 2010. Jurassic arc volcanism on Crimea (Ukraine): implications for the paleo-subduction zone configuration of the Black Sea region. *Lithos* 119, 412—426. doi: 10.1016/j.lithos.2010.07.017.
- Mileev V. S., Baraboshkin E. Yu., Rozanov S. B., Rogov M. A., 2006. Cimmerian and Alpine tectonics of the Crimea mountains. *Bulletin of the Moscow Society of Naturalists, Department of Geology* 81, 22—33 (in Russian).
- Munteanu I., Matenco L., Dinu C., Cloetingh S., 2011. Kinematics of back-arc inversion of the Western Black Sea Basin. *Tectonics* 30, TC5004. doi: 10.1029/2011TC002865.
- Munteanu I., Willingshofer E., Sokoutis D., Matenco L., Dinu C., Cloetingh S., 2013. Transfer of deformation in back-arc basins with a laterally variable rheology: Constraints from analogue modelling of the Balkanides—Western Black Sea inversion. *Tectonophysics* 602, 223—236. doi: 10.1016/j.tecto.2013.03.009.
- Muratov M. V., 1960. Brief outline of the geological structure of the Crimean peninsula. Moscow: State Scientific and Technical Publishing House of Literature on Geology and Conservation of Subsoil, 217 p. (in Russian).
- Muratov M. V., Sydorenko A. V. (eds.), 1969. Geology of the USSR. Vol. 8. Geological Description. Crimea. Moscow: Nedra, 576 p. (in Russian).

- Nikishin A. M., Korotaev M. V., Ershov A. V., Brunet M. F., 2003. The Black Sea basin: tectonic history and Neogene-Quaternary rapid subsidence modeling. *Sediment. Geol.* 156, 149—168. doi: 10.1016/S0037-0738(02)00286-5.
- Nikishin A. M., Okay A. I., Tüysüz O., Demirel A., Amelin N., Petrov E., 2015a. The Black Sea basins structure and history: New model based on new deep penetration regional seismic data. Part 1: Basins structure and fill. *Mar. Petrol. Geol.* 59, 638—655. doi: 10.1016/j.marpetgeo.2014.08.017.
- Nikishin A. M., Okay A. I., Tüysüz O., Demirel A., Amelin N., Petrov E., 2015b. The Black Sea basins structure and history: New model based on new deep penetration regional seismic data. Part 2: Tectonic history and paleogeography. *Mar. Petrol. Geol.* 59: 656—670. doi: 10.1016/j.marpetgeo.2014.08.018.
- Nikishin A. M., Wannier M., Alekseev A. S., Al-mendinger O. A., Fokin P. A., Gabdullin R. R., Khudoley A. K., Kopaevich L. F., Mityukov A. V., Petrov E. I., Rubtsova E. V., 2015c. Mesozoic to recent geological history of southern Crimea and the Eastern Black Sea region. *Geol. Soc. London Spec. Publ.* 428. doi: 10.1144/SP428.1.
- Nikishin A. M., Ziegler P. A., Panov D. I., Nazarevich B. P., Brunet M. F., Stephenson R. A., Bolotov S. N., Korotaev M. V., Tikhomirov P. I., 2001. Mesozoic and Cainozoic evolution of the Scythian Platform-Black Sea-Caucasus domain. In: *Peri-Tethys Memoir 6: Peri-Tethyan Rift/Wrench Basins and Passive Margins*. Paris: Mémoires du Muséum national d'Histoire naturelle, 186, P. 295—346.
- Oszczypko N., Slaczka A., Bubniak I., Olszewska B., Garecka M., 2017. The position and age of flysch deposits in the Crimea Mountains (Southern Ukraine). *Geological Quarterly* 61(4), 697—722. doi.org/10.7306/gq.1359.
- Pánek T., Danišík M., Hradecký J., Frisch W., 2009. Morphotectonic evolution of the Crimean mountains (Ukraine) as constrained by apatite fission track data. *Terra Nova* 12(4), 271—278. doi: 10.1111/j.1365-3121.2009.00881.x.
- Reilinger R., McClusky S., Vernant P., Lawrence S., Ergintav S., Cakmak R., Ozener H., Guliev F. K. I., Stepanyan R., Nadariya M., Hahubia G., Mahmoud S., Sakr K., ArRajehi A., Paradissis D., Al-Aydrus A., Prilepin M., Guseva T., Evren E., Dmitrova A., Filikov S. V., Gomez F., Al-Ghazzi R., Karam G., 2006. GPS constraints on continental deformation in the Africa-Arabia-Eurasia continental collision zone and implications for the dynamics of plate interactions. *J. Geophys. Res.* 111, B05411. doi: 10.1029/2005JB004051.
- Robinson A. G., Rudat J. H., Banks C. J., Wiles R. L. F., 1996. Petroleum geology of the Black Sea. *Mar. Petrol. Geol.* 13(2), 195—223. [https://doi.org/10.1016/0264-8172\(95\)00042-9](https://doi.org/10.1016/0264-8172(95)00042-9).
- Saintot A., Angelier J., Chorowicz J., 1999. Mechanical significance of structural patterns identified by remote sensing studies: a multiscale analysis of tectonic structures in Crimea. *Tectonophysics* 313(1-2), 187—218. doi: 10.1016/S0040-1951(99)00196-1.
- Saintot A., Stephenson R. A., Stovba S., Brunet M. F., Yegorova T., Starostenko V., 2006. The evolution of the southern margin of eastern Europe (Eastern European and Scythian platforms) from the latest Precambrian-Early Palaeozoic to the Early Cretaceous. *Geol. Soc. London. Memoirs* 32, 481—505. doi: 10.1144/GSL.MEM.2006.032.01.30.
- Schmid S. M., Bernoulli D., Fügenschuh B., Matenco L., Schefer S., Schuster R., Tischler M., Ustaszewski K., 2008. The Alpine-Carpathian-Dinaridic orogenic system: correlation and evolution of tectonic units. *Swiss J. Geosci.* 101, 139—183. doi 10.1007/s00015-008-1247-3.
- Sheremet Y., Sosson M., Muller C., Gintov O., Murovskaya A., Yegorova T., 2016a. Key problems of stratigraphy in the Eastern Crimea Peninsula: some insights from new dating and structural data. *Geol. Soc. London Spec. Publ.* 428. doi: 10.1144/SP428.14.
- Sheremet Y., Sosson M., Muller C., Gintov O., Murovskaya A., Yegorova T., 2016a. Key problems of stratigraphy in the Eastern Crimea Peninsula: some insights from new dating and structural data. *Geol. Soc. London Spec. Publ.* 428. doi: 10.1144/SP428.14.
- Sheremet Y., Sosson M., Ratzov G., Sydorenko G., Voitsitskiy Z., Yegorova T., Gintov O., Murovskaya A., 2016b. An offshore-onland transect across the north-eastern Black Sea basin (Crimean margin): Evidence of Paleocene to Pliocene two-stage compression. *Tectonophysics* 688, 84—100. doi: 10.1016/j.tecto.2016.09.015.
- Slavin V. I., 1989. Geological evolution of the

- Crimea in the Mesozoic. *Bulletin of Moscow University. Ser. Geology* (6), 24—36 (in Russian).
- Smolyaninova E. I., Mikhailov V. O., Lyakhovskiy V. A., 1996. Numerical modelling of regional neotectonic movements in the northern Black Sea. *Tectonophysics* 266(1-4), 221—231.
- Solov'ev A. V., Rogov M. A., 2010. First fission-track dating of zircons from Mesozoic complexes of the Crimea. *Stratigr. Geol. Correl.* 18(3), 298—306. doi.org/10.1134/S0869593810030068.
- Starostenko V., Janik T., Stephenson R., Gryn D., Rusakov O., Czuba W., Środa P., Grad M., Guterch A., Flüh E., Thybo H., 2016. DOBRE-2 WARR profile: the Earth's upper crust across Crimea between the Azov Massif and the north-eastern Black Sea. *Geol. Soc. London Spec. Publ.* 428(1), 199—220. doi: 10.1144/SP428.11.
- Starostenko V., Janik T., Yegorova T., Farfuliak L., Czuba W., Środa P., Thybo H., Artemieva I., Sosson M., Volfman Y., Kolomiyets K., Lysynchuk D., Omelchenko V., Gryn D., Guterch A., Komminaho K., Legostaeva O., Tiira T., Tolkunov A., 2015. Seismic model of the crust and upper mantle in the Scythian platform: the DOBRE-5 profile across the north western Black Sea and the Crimean peninsula. *Geophys. J. Int.* 201(1), 406—428. doi: 10.1093/gji/ggv018.
- Stephenson R. A., Mart Y., Okay A., Robertson A. H. F., Saintot A., Stovba S., Kriachtchevskaia O., 2004. Transect VIII: Eastern European Craton to Arabian Craton (Red Star to Red Sea). In: *The TRANSMED Atlas — the Mediterranean Region from Crust to Mantle*. Vol. XXIII. Berlin: Springer, 120—127.
- Sydorenko G., Stephenson R., Yegorova T., Starostenko V., Tolkunov A., Janik T., Majdanski M., Voitsitskiy Z., Rusakov O., Omelchenko V., 2016. Geological structure of the northern part of the Eastern Black Sea from regional seismic reflection data including the DOBRE-2 CDP profile. *Geol. Soc. London Spec. Publ.* 428, 307—321. doi: 10.1144/SP428.15.
- Tchaikovskiy B., Biletskyi S., Deev S., Demjan O., Krasnorudskaya S., 2006. Ukrainian State Geological Map of L-36-XXVIII and L-36-XXXIV (1:200000 scale). Crimea region, State Geological Survey (in Ukrainian).
- Vakarchuk S., Kharchenko M., Bezkhlyzhko O., Shevchenko O., Kuzmenko P., Bashkirov G., Ishchenko I., Kitchka A., 2016. The discovery of the Subbotin oil field offshore Ukraine: Geological challenges and exploration lessons. Conference: *Petroleum Systems of Alpine-Mediterranean Fold Belts and Basins, AAPG European Region Conference & Exhibition, At Bucharest 19—20 May, 2016*, P. 32—33.
- Vincent S. J., Carter A., Lavrishchev A., Price S. P., Barabadze T. G., Hovius N., 2010. The exhumation of the western Greater Caucasus: A thermochronometric study. *Geol. Mag.* 148(1), 1—21. doi: 10.1017/S0016756810000257.
- Vincent S. J., Morton A. C., Carter A., Gibbs S., Barabadze T. G., 2007. Oligocene uplift of the western Greater Caucasus: An effect of initial Arabia-Eurasia collision. *Terra Nova* 19(2), 160—166. doi: 10.1111/j.1365-3121.2007.00731.x.
- Yegorova T., Gobarenko V., 2010. Structure of the Earth's crust and upper mantle of West and East Black Sea Basins revealed from geophysical data and its tectonic implications. In: *Sedimentary Basin Tectonics from the Black Sea and Caucasus to the Arabian Platform*. *Geol. Soc. London Spec. Publ.* 340, 23—42. doi: 10.1144/SP340.3.